Evaluating Cutting Fluid Effects on Cylinder Boring Surface Errors by Inverse Heat Transfer and Finite Element Methods

Y. Zheng

H. Li

W. W. Olson

J. W. Sutherland

Dept. of Mechanical Engineering—
Engineering Mechanics,
Michigan Technological University,
1400 Townsend Drive,
Houghton, MI 49931

Sets of dry and wet boring experiments are conducted to estimate the amount of heat transferred into the workpiece and the cutting fluid heat convection coefficient in a boring operation by an inverse heat transfer method. The temperature distribution in the bore is predicted using a heat transfer model that includes heat convection on the inner and outer bore walls. The developed model is solved by an integral transform approach. The thermal expansion of the bore is then calculated using the finite element method (FEM). Surface error due to the cutting forces is also predicted using FEM and added to the thermally induced surface error to give the total surface error. The actual surface error of bores machined under dry and wet cutting conditions are measured and compared with the predicted surface error. Very good agreement between measured and predicted surface errors is observed. [S1087-1357(00)00802-9]

Introduction

Manufacturers are devoting more and more attention to the various waste streams generated in metal cutting operations under the pressure of increasing disposal costs and tighter environmental regulations. Spent cutting fluid is one of the most significant waste streams in manufacturing facilities. In spite of their importance, there is a shortage of knowledge about the effects of cutting fluids on cutting performance. This paper begins to address this shortage of knowledge by quantifying the role that cutting fluids play in removing heat from the workpiece during a cylinder boring operation. The impact of cutting fluids on the machined workpiece surface error is also determined.

The study considers an Al 308 work material because of the widespread use of cast aluminum alloys in the automotive industry. A cylinder boring process is examined owing to its common use in engine manufacture. It is known that the lack of cylindricity of bores often leads to poor engine performance because of increased oil consumption, frictional losses, and excessive wear of piston rings. Among all the machined surface features, e.g., surface error, surface waviness and surface roughness, the surface error is the most critical factor affecting the cylindricity of the machined bores, and will be addressed in this work.

Surface error is defined as a measure of the deviation of the machined surface from the surface that would be produced under ideal conditions [1]. Surface error is mainly caused by the elastic deflection of the bore due to cutting forces and the thermal deformation of the bore due to the heat generated during machining.

Obviously, the cutting force induced surface error depends on the magnitude and direction of the cutting force, the bore structure, as well as the mechanical properties of the bore material. The cutting forces may be easily measured using a dynamometer or predicted by applying some widely used models [2–4]. In this effort, the cutting forces are measured directly from experiments.

The thermal deformation of a machined bore is a function of the temperature distribution in the bore. The temperature distribution in the bore is in turn dependent on the i) heat source strength, ii) bore structure, iii) thermophysical properties of the work material, and iv) convective boundary conditions. The convective boundary conditions on the walls of the bore are controlled by the fluid properties and the conditions under which the fluid is applied. One model for predicting the heat convection coefficient was presented by Childs et al. [5] that considered the local behavior near the cutting zone and assumed heat loss by boiling. Such a model does not adequately describe the global convection behavior in a boring operation. In fact, no theoretical correlation for the heat convection coefficient in cylinder boring is available due to the complexity of the cutting fluid flow pattern and the uncertainty of cutting fluid application [6].

With regard to the heat source strength, a number of experimental and theoretical efforts have focused on determining the amount of process generated heat that is distributed to the chips, tool, and workpiece, and the effect that the cutting conditions have on this distribution [7,8]. The literature reports that under typical cutting conditions, the majority of the heat is carried away by the chips, with only 10–30 percent of the heat conducted into the workpiece. Subramani [9] employed an inverse heat transfer method to estimate that as much as 46 percent of the generated heat may be transferred into a cast iron bore. Wright et al. [10,11] also applied an inverse heat transfer method to solve for the tool/chip interface temperature in turning based on temperature measurements on the interior of the tool. The research to be reported herein also utilizes an inverse heat transfer method to estimate the heat source strength for a set of dry boring experiments on 308 aluminum. It is anticipated that the fraction of the heat transferred into the bore may be larger than that observed for a cast iron bore owing to the higher conductivity of aluminum relative to cast iron.

Several researchers have examined the temperature distributions and thermal distortions created by machining processes. Watts and McClure [12] analyzed the thermal expansion of a workpiece by assuming a linearly moving ring heat source in turning. Watts [13] presented the temperature distributions in solid and hollow cylinders due to a moving circumferential ring heat source. Ichimiya and Kawahara [14] also focused on turning and instead of assuming a ring heat source, employed a helically moving point heat source. Stephenson [15,16] developed an inverse method for investigating deformation zone temperatures and the thermal expansion of the workpiece in turning. With regard to cylinder boring, Kakade and Chow [17] simulated the bore distortions due to both the mechanical deflection and thermal expansion using the finite element method. However, no experimental vali-

dation of the model predictions were made. A model has also been developed for the prediction of bore surface error that includes the effects of both cutting forces and bore temperature [1,3,9]. The comparisons between the experimental measurements and the model predicted surface error showed good agreement. However, the effect of cutting fluid on the surface error was not considered in their work.

This paper focuses on predicting the surface error resulting from a boring operation performed both with and without cutting fluid. Cutting forces and temperatures are measured for both dry and wet boring tests. The temperature measurements under various cutting conditions are used to determine the actual heat source strength as well as the cutting fluid heat convection coefficient by an inverse heat transfer method. A one-dimensional heat transfer model is developed to simulate the heat transfer process in the bore with two-sided cooling by the cutting fluid. The integral transformation method is used to solve the heat transfer problem [18,19]. The deflection of the bore due to the measured cutting forces and the thermal expansion of the bore as a function of the temperature field in the bore are calculated using a finite element model. These predicted (combined thermal and mechanical) surface errors are then compared with the measured errors at a number of axial positions in the bore.

Cutting Force and Temperature Measurements

A set of boring tests were performed using 308 die cast aluminum workpieces on a Cincinnati Milacron Vertical Machining Center (7VMC-750). The variables investigated in the experiment included cutting speed, feed, and cutting fluid presence. The cutting conditions for the experiments formed a 2^3 factorial design. Tests 1–4 were conducted dry whereas tests 5–8 were performed in the presence of cutting fluid. The depth of cut was fixed at 1 mm (0.04 inch) for all the tests. For each test, the cutting forces and the transient temperature responses at five different thermocouple locations were measured simultaneously.

The experimental setup is shown in Fig. 1. The tooling for the operation was a boring bar (70 mm diameter, 150 mm length) with an indexable tool cartridge (Kennametal 55946 C-A-5). The cutting fluid used for the tests was a water soluble oil at 10 percent concentration. A cutting fluid flow rate of 7.5 l/min. (1.98 gal/min.) was applied via several nozzles directed at the top of the cylinder.
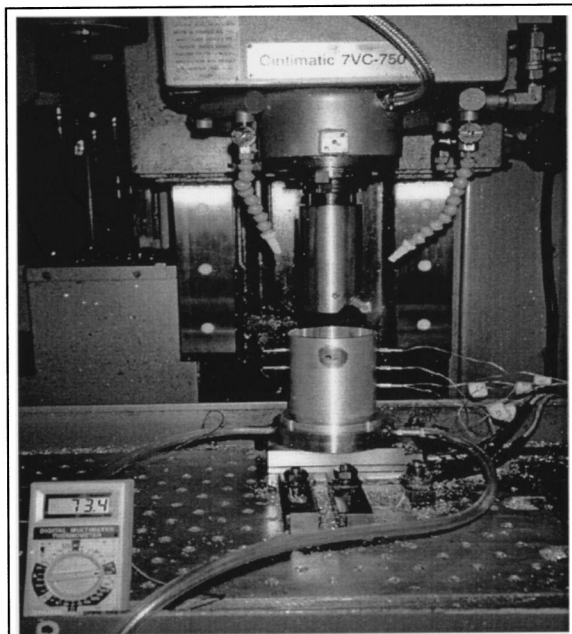
Cutting Force Measurement. A Kistler dynamometer (Model 9257A) was used to measure the three components of the cutting force. A multi-channel charge amplifier (Kistler Type 5001) received the dynamometer output and supplied voltages to the data acquisition system (AT-MIO-15F DAQ board and Lab View software system). The measured cutting forces were subsequently input to the finite element model to predict elastic deflections. To check the repeatability of the force measurements, known loads were applied to the dynamometer, and the corresponding voltages were noted. Repeated application of a known load resulted in virtually the same voltage.

Temperature Measurement. Coaxial thermocouples of type E (Medtherm Corporation), were used in the tests. This type of thermocouple was selected because its fast response time of 10 microseconds can be used to capture transient temperature behavior at high cutting speeds (1000–3000 rpm).

Temperature measurements were taken at five positions continuously during the boring operation. A schematic of a cylinder bore with the five mounted thermocouples is shown in Fig. 2. All the cylinder bores were prepared with the same outer and inner diameters. Two main modifications were made to the cylinders. One was to cut a 3.2 mm. (0.125 inch) square slot along the full length of the inside surface of the cylinders so that the angular orientation of the boring bar could be matched with the cutting force signals. Another modification was to drill five holes, each of 2.1 mm (0.082 inch) diameter, as shown in Fig. 2, into which the thermocouples were mounted. The holes at locations A and B were at the same distance of 25.4 mm (1 inch) from the top of the bore, but at different radial and angular (180 deg apart) locations. The holes at locations C and D were created in a similar fashion. Hole E is at the same radial and angular location as B and D. A conductive paste was applied at the bottom of each hole to ensure adequate contact between the thermocouple probe tip and the bore wall.

The data acquisition system for temperature measurement in the tests consisted of a National Instruments chassis SCXI-1000, a data controller SCXI-1200, an isolation amplifier SCXI-1120, and LabView 4.0 software. The thermocouples were connected to the SCXI-1120 modules using SCXI-1328 terminal blocks. The terminal block included a temperature sensor for cold-junction compensation. Due to the small magnitudes of the output voltages from the thermocouples, signal conditioning was required before A/D conversion.

It will be seen that the temperature history collected from the thermocouples for each test will be used to estimate the heat source strength and the boundary heat convection coefficient by the inverse heat transfer method. Typical temperature histories obtained for dry and wet machining are shown in Figs. 3(a) and 3(b) respectively. The figures illustrate that the cutting fluid has a

Fig. 1 Picture of the experimental setup
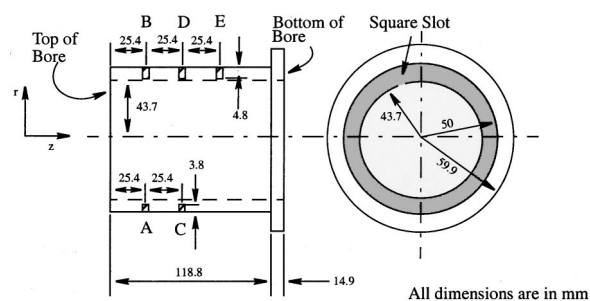
Fig. 2 Schematic of a cylinder bore with mounted thermocouples
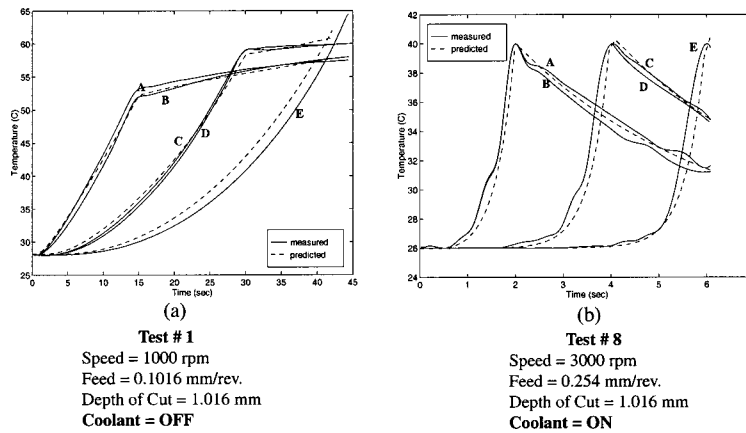
Fig. 3 Predicted and measured temperatures for tests # 1 & # 8

significant effect on the temperature in the bore. These differences in the temperature history suggest differences in the bore thermal deformations that will be explored later. The temperature history at locations ''A'' and ''B'' (also ''C'' and ''D'') which are at the same axial location, but different radial and circumferential locations reveals that the temperature measurements are consistent.

Heat Transfer Model for Cylinder Boring

As a first step in predicting the thermal deformation in the cylinder boring process, a model for the heat transfer behavior in the operation is required. A comparison of the thermocouple measurements at the same axial position, but different radial positions, i.e., thermocouple pairs A/B, and C/D, reveals that the temperature difference between them is not significant. The relatively small temperature difference of 2°C between the thermocouple pairs is due to the very high thermal conductivity of the aluminum workpiece, 120.0 W/m · K, the thin cylinder walls, 6.35 mm (0.25 inch), and the relatively high spindle speeds. The lag/lead between the temperatures at A & B; and C & D, is also observed to be negligible. These two observations suggest that from a modeling perspective, the radial temperature and circumferential temperature gradients are small and may be neglected. This dramatically simplifies the modeling of the heat transfer problem, leading to a one-dimensional heat transfer model with a heat convection term associated with cooling on the inside and outside of the bore walls. In contrast to our results, a circumferential temperature gradient was observed in the study conducted by Subramani [9], but that can be attributed to the lower conductivity and thick wall of the cast iron cylinder used.

Governing Equation and Boundary Conditions. Figure 4, illustrates the one-dimensional governing equation of the heat

transfer problem in a cylindrical bore. This equation, that incorporates a longitudinally moving heat source and heat losses through the inside and outside of the bore walls, takes the following form:

$$w\frac{d^2\theta}{dz^2} - 2H\theta + \frac{g(z,t)}{k} = \frac{w}{\alpha}\frac{\partial\theta}{\partial t} \qquad (1)$$

where; θ is the difference between the wall temperature and the ambient temperature, α is the thermal diffusivity of the material, k is the thermal conductivity, H is the ratio of heat convection coefficient to thermal conductivity, i.e., $H = h/k$, w is the thickness of the wall of the bore, and $g(z,t)$ is the heat source strength. Equation (1) is subjected to the following boundary and initial conditions:

$$\frac{\partial\theta}{\partial z} \mp H\theta = 0 \quad \text{at } z = 0, \quad \text{and } L \text{ respectively}$$

$$\theta = 0 \quad \text{at } t = 0, \quad \text{for all } z. \qquad (2)$$

The heat source strength at cutting tool position z_s in the boring operation may be approximated by:

$$g(z_s,t) = g_s \cdot \delta(z - z_s) \qquad (3)$$

where; z_s may be further expressed in terms of the feedrate (F), time (t), and the initial position (z_0) of the tool, i.e., $z_s = z_0 + Ft$. For the experiments described herein, z_0 correspond to the top position of the cylinder, i.e., $z = 0$.

Temperature Solution via Integral Transformation. There are many ways to obtain the solution of Eq. (1) subjected to the initial and boundary conditions of Eq. (2). The integral transfor-
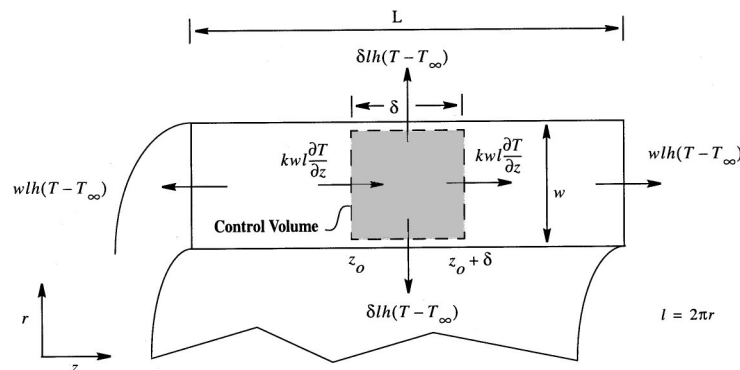
Fig. 4 Cylinder bore illustrating heat loss terms

mation approach is applied herein [18,19]. The kernel of the integral transform in the z-direction, $K_n(\lambda_n,z)$, and the corresponding eigenvalues, λ_n may be expressed as [19,22]:

$$K_n(\lambda_n,z)=\sqrt{2}\cdot\frac{\lambda_n\cos(\lambda_n z)+H\sin(\lambda_n z)}{\left[(\lambda_n^2+H^2)\left(L+\dfrac{H}{\lambda_n^2+H^2}\right)+H\right]^{1/2}} \quad (4)$$

$$\tan\lambda_n L=\frac{2\lambda_n H}{\lambda_n^2-H^2} \quad (5)$$

where L is the length of the bore.

The integral transformation of Eq. (1) results in an ordinary differential equation. The solution for this equation is:

$$\bar{\theta}(\lambda_n,t)=\frac{\alpha\cdot g_s}{wk}\cdot\frac{\psi_1+\psi_2+\psi_3}{\gamma_n^2+\lambda_n^2 F^2} \quad (6)$$

where $\bar{\theta}$ is the transformed temperature, and the variables ψ_1, ψ_2, and ψ_3 may be defined as:

$$\psi_1=e^{-\gamma_n t}(B\lambda_n F-A\gamma_n),$$

$$\psi_2=\sin(\lambda_n Ft)(A\lambda_n F+B\gamma_n),\ \ \text{and}$$

$$\psi_3=\cos(\lambda_n Ft)(A\gamma_n-B\lambda_n F).$$

The constants in the above definitions for ψ_1, ψ_2, and ψ_3 are:

$$\gamma_n=\alpha(2H+w\lambda_n^2)/w,$$

$$A=\lambda_n\cos(\lambda_n z_0)+H\sin(\lambda_n z_0),\ \ \text{and}$$

$$B=H\cos(\lambda_n z_0)-\lambda_n\sin(\lambda_n z_0).$$

Given the transformed temperature relationship of Eq. (6) and the values for the variables specified above, the temperature distribution in the cylinder bore may be calculated using the inverse integral transformation, i.e.,

$$T(z,t)=\sum_{n=0}^{\infty}K_n(\lambda_n,z)\bar{\theta}(\lambda_n,t)+T_\infty \quad (7)$$

where T_∞ is the ambient temperature.

Prediction of Heat Source Strength and Convection Coefficients

Due to the lack of models for predicting the heat source strength and convection coefficient in cylinder boring, as mentioned in the literature review, an inverse heat transfer method was used to estimate these quantities based on the measured temperature history from the thermocouples. This inverse heat transfer method uses an objective function that is the sum of the squared deviations of the model predicted temperatures from the measured temperatures. The squared deviations are summed over all the thermocouples for the duration of the boring operation. Given the thermocouple measurements from a boring operation, values of the heat source strength and convection coefficient are identified that minimize the objective function. Of course, this inverse heat transfer method assumes that the heat source strength and convection coefficient are constant for the duration of a boring operation. In a boring process without cutting fluid, and slow motion of air around the cylinder, a heat convection coefficient of 6 W/m^2 K was assumed [6].

Table 1 lists the machining conditions, the estimated heat source strength, the fraction of total energy entering the workpiece, and the convection coefficients for the eight tests conducted. Tests 1–4, were conducted in the absence of cutting fluid, i.e., dry. Assuming the heat convection coefficient to be 6 W/m^2 K for these dry tests, the heat source strength was determined using the inverse heat transfer approach for each case. The power consumed or the total heat produced in each test was known (product of measured cutting force and cutting speed). So, the fraction of total heat energy entering the workpiece was determined. For the conditions examined, the heat fraction was in the range of 0.26–0.77. Tests 5–8, were conducted in the presence of cutting fluid, i.e., wet. The heat source strengths in tests 5–8, were assumed to be the same as those determined in the corresponding dry tests 1–4. For example, the heat source strength in tests 5 and 1 was assumed to be the same. Obviously, the heat fraction entering the workpiece would also be the same in corresponding dry and wet tests, since the cutting forces remained virtually unchanged in the presence and absence of the cutting fluid. Once again, the inverse heat transfer approach was applied and the convection coefficients for the wet tests 5–8, were determined. The convection coefficients estimated for the listed machining conditions were in the range of 1400–2100 W/m^2 K. It should be noted that the convection coefficients estimated were global, as compared to local convection coefficients estimated by Childs [5].

Figures 3a and 3b show the temperature history at the thermocouple locations for a typical dry and wet test respectively. A good agreement between model and experiment is observed in terms of the trend of the temperature history, which shows that the model has been able to adequately characterize the physics of the problem. So, it can be concluded that the developed one-dimensional heat transfer model with side heat losses is acceptable to simulate the process of boring a thin walled cylinder of highly conductive material in the presence and absence of the cutting fluid.

Cylinder Boring Surface Error

For the bore geometry outlined previously and the specified depth of cut, and in the absence of deformations, it would be

Table 1 Estimated heat source strength and convection coefficient

Test #	Feed (mm/rev)	Spindle Speed (rpm)	Coolant	Estimated Heat Source Strength (W)	Estimated Fraction of Total Heat Entering the Workpiece	Estimated Convection Coefficient (W/m²K)
1	0.1	1000	OFF	858.5	0.767	6
2	0.254	1000	OFF	896.13	0.475	6
3	0.1	3000	OFF	1596.9	0.435	6
4	0.254	3000	OFF	1496.2	0.271	6
5	0.1	1000	ON	858.5	0.767	2014
6	0.254	1000	ON	896.13	0.475	1561
7	0.1	3000	ON	1596.9	0.435	1496
8	0.254	3000	ON	1496.2	0.271	1575

expected that a cylinder diameter of 89.4 mm would be produced. Of course, cutting forces might be expected to separate the boring bar and the bore wall. This would reduce the depth of cut leading to an undersized machined diameter, i.e., surface error. Elevated temperatures in the cylinder bore would also be expected to produce thermal deformations of the bore that result in a reduced diameter and hence surface error. Residual stresses in the machined workpiece can also lead to surface error. However, the literature reports that for machining conditions comparable to those described above, the residual stresses are small and do not lead to significant distortions [20,21].

Force-Induced Errors. The deflection of the boring bar and the cylinder bore due to the cutting forces leaves an uncut layer of material in the radial direction, which contributes to the surface error of the bore. For the conditions considered, the stiffness of the boring bar is much larger than that of the bore. The deflection of the boring bar due to the cutting forces can be determined by modelling it as a cantilever beam. It was found to be in the range of 0.1–0.3 microns for the measured cutting forces during the tests.

The elastic deflection of the bore resulting from the cutting forces in the boring operation is computed by the finite element approach. The following boundary conditions were assumed for the force analysis of the cylinder:

i) Fixed at $z=L$
ii) Free at $z=0$

The distortion of the bore, 10 seconds after the cutting had started, is shown in Fig. 5. Note that the expansion shown in this figure is exaggerated for illustration purposes. The finite element model consisted of 600 solid elements and 880 nodes.

Since the tool is moving during machining, the point of application of the cutting forces on the bore varies with time. Finite element analysis was performed at several different points. The surface errors (bore deflection at the point of surface generation) due to ''cutting forces only,'' at several axial positions were obtained and plotted in Fig. 6 for the cutting conditions of test #1. The maximum surface error of the bore is about 2.4 microns, which is much higher than that of the boring bar (0.2 microns). Therefore, the surface error contribution due to the boring bar deflection has been neglected. The surface error resulting from the cutting force during machining is only one part of the total surface error in the machined bore.

Thermally Induced Errors. Another significant source contributing to the total surface error on the bore is the thermal expansion of the work piece due to the heat generated during machining. In order to evaluate the pure effect of the cutting fluid on the surface error, the results for both dry and wet machining will be presented. Among the boring bar, cartridge, and the insert, only the insert is subjected to high temperature. The cutting operation is not long enough for the bar and cartridge to become appreciably heated. Calculations revealed that the expansion of the insert in

the radial direction was small (in the range of 0.4–0.6 microns). Therefore, only the thermal expansion of the bore is considered.

Based on the aforementioned heat transfer and inverse heat transfer methods, the temperature distributions in the axial direction in the workpiece at 10, 20, 30, and 40 seconds after process initiation are shown in Fig. 7a and 7b.

At time $t=10$ s, the thermal expansion of the bore is shown in Figs. 8 and 9. Note that the expansion shown in Figs. 8a and 8b has been exaggerated. Due to the symmetry of the bore and the thermal expansion, only side views are presented in Figs. 9a and 9b. The data for these graphs were obtained using finite element method.

These figures show that not only is the magnitude of surface error in machining in the presence of cutting fluid smaller than that without cutting fluid, but also the surface error in wet cutting is more uniformly distributed in the axial direction of the bore compared with that in dry cutting. This was found true for all the bores machined in the presence of the cutting fluid. In either case, the thermal expansion, rather than the elastic deflection resulting from the cutting forces, is the dominant factor in influencing the surface error on the machined bore. In considering the magnitude of the surface error produced under wet conditions, it should be noted that the jet cooling method was used as opposed to the flood
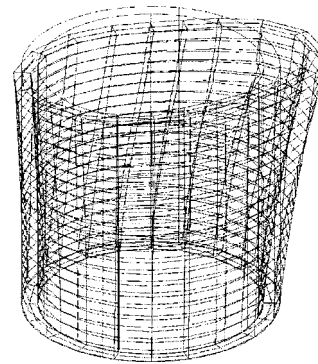
Fig. 5 Deformed cylinder at $t=10$ seconds due to the cutting forces, test #1
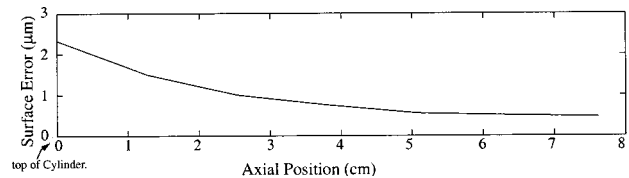
Fig. 6 ''Force-induced'' surface error vs. axial position in the bore for test #1

(a) Test # 1, Without Cutting Fluid   (b) Test # 8, With Cutting Fluid
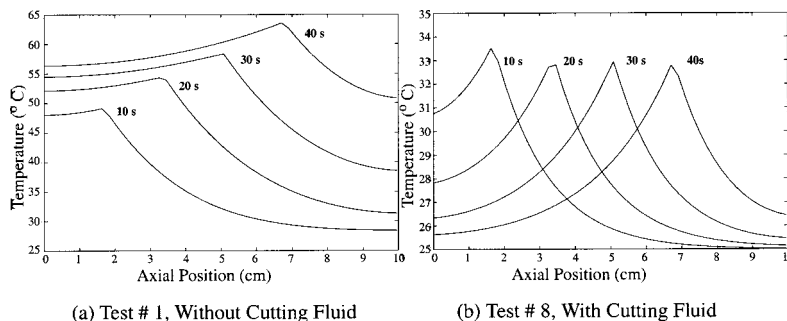
Fig. 7 Predicted temperature distribution in the bore at different times

(a) Test # 1, Without Cutting Fluid   (b) Test # 8, With Cutting Fluid
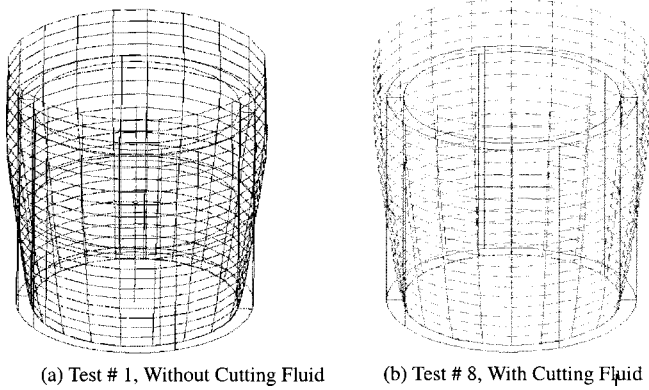
Fig. 8 Deformed bore due to the thermal deformation at $t=10$ second

cooling method. Perhaps, with flood cooling, the reduction in the surface error would have been greater. Clearly, additional research is needed to understand the effect of coolant application strategy (coolant flow rate, number of nozzles, nozzle direction, nozzle diameter, distance between nozzle and cutting zone, etc.) on the surface error of the workpiece.

Comparison of Measured and Model Predicted Surface Errors. A Brown & Sharpe Micro Validator Series Coordinate Measuring Machine (CMM) was used to measure the surface error on the machined bores. When the pick-up of a measuring probe in this system touches and moves around the inner surface of the machined bore at a given axial position, the digitized contour of the inner surface of the bore at the axial position is obtained. The software provided with this measurement system is able to calculate the average radius of this contour. The difference

between the desired radius and this measured radius is surface error; positive surface error is associated with an undersized machined diameter.

In Fig. 10, the measured surface error is compared with the combined predicted surface error, which is contributed by both the elastic deflection due to the cutting forces and the thermal expansion resulting from the heat generated in machining. The measured surface error is slightly greater than the combined predicted error. The difference between the two may be due to the combined effects of boring bar deflection, residual stresses and surface roughness. A good agreement between the predicted and the measured values suggests that the developed procedure to predict the surface error on the machined bore by a boring operation in the presence and absence of cutting fluid is successful. Other tests also showed equally good agreement between the measured and the predicted surface error. To verify the repeatability of the CMM, repeated measurements of the diameter at an axial position were taken on a machined cylinder. The measurements revealed a standard deviation of 1.2 microns in the diameter, which is very small relative to the surface error values.

Conclusions

Manufacturers are devoting increased attention to cutting fluids because of the environmental and health consequences associated with their usage. Many recent studies have focused on these negative characteristics, but little attention has been directed at describing the effects of cutting fluids on machining process performance. The emphasis of this paper has been on quantifying the role that cutting fluid application has on convective heat transfer and machined surface error in a cylinder boring operation. A one dimensional model for heat transfer in the boring operation that can be used for both dry and wet cutting was established and verified experimentally. Measured temperatures were used in concert with an inverse heat transfer method to estimate heat source strengths for dry cutting and convection coefficients for wet cutting.

(a) Test # 1, Without Cutting Fluid   (b) Test # 8, With Cutting Fluid
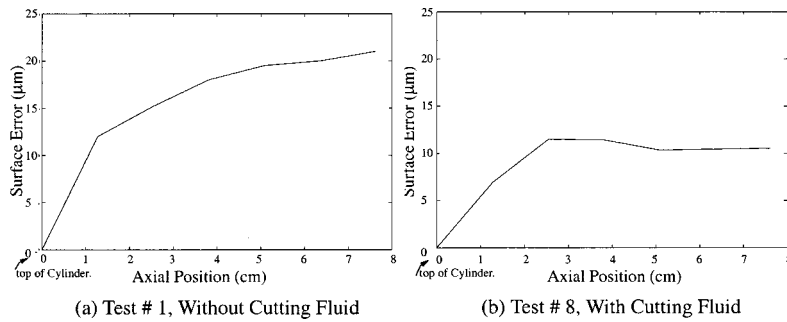
Fig. 9 Surface error (due to thermal deformation) versus axial position based on FEM model

(a) Test # 1, Without Cutting Fluid   (b) Test # 8, With Cutting Fluid
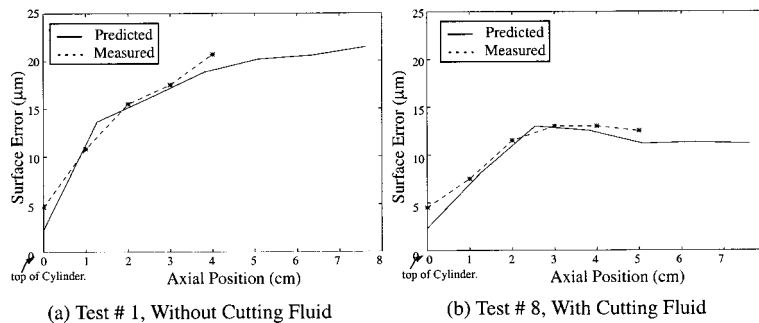
Fig. 10 Measured surface error versus predicted (elastic+thermal) surface error

The predicted temperature fields produced in the cylinder bore create thermal deformations. The cutting forces also generate deformations. The predicted temperature fields and the measured cutting forces were both input to a finite element model of the cylinder bore, and the bore surface errors were calculated. The predicted bore surface errors under a variety of dry and wet machining conditions were then compared to measured bore surface errors produced under like machining conditions. These comparisons showed good agreement between the model predicted and measured surface errors. The following conclusions may be drawn as a result of this investigation:

• The amount of heat transferred into the workpiece under dry boring conditions ranges from 27–77 percent of the total heat generated.
• A one-dimensional heat transfer model for the cylinder boring process adequately describes the measured temperature behavior for the conditions examined.
• Surface errors developed from a finite element model of the bore and applied cutting forces/temperature field adequately describe measured surface errors.
• Convection coefficients obtained via inverse heat transfer method under the application of cutting fluid revealed coefficients approximately three orders of magnitude higher than for dry cutting (1500 W/m^2 K versus 6 W/m^2 K).
• For the conditions examined, the thermal deformations dominate the deformations due to the cutting forces (90 percent versus 10 percent for dry machining and 85 percent versus 15 percent for wet machining).
• Since the thermal deformations dominate for the conditions examined, and since the temperature of the bore increases during the operation, the machined diameter tends to be smaller at the bottom of the bore than at the top.
• For the conditions considered, the surface error tends to increase throughout the bore (i.e., from top to bottom) for dry cutting. For wet cutting, the surface error increases initially, but then flattens out—near the bottom of the bore, the surface error is nearly constant.
• The introduction of cutting fluid reduces the surface error from that produced in dry boring by approximately one half.

While this last point demonstrates the importance of cutting fluid to a cylinder boring operation, it should be noted that under different conditions, e.g., different work material/geometry and fluid application conditions (flow rate, pressure, etc.), the cutting fluid effect could be more or less dramatic. So, for every case, process decision makers should evaluate the relative merits of the fluid and judge whether its benefits outweigh its liabilities.

Finally, the efforts described herein have focused on a relatively simple situation, so as to avoid complexities that could obscure/confuse the cutting fluid effect. Certainly, a similar 2D or 3D heat conduction model can be developed for thick walled cylinders of lower conductivity. However, it would require complex numerical methods leading to slow convergence of the minimization procedures.

Acknowledgments

Nomenclature

α = thermal diffusivity, m^2/s
F = feed rate, m/s
g_s = point heat source, W
h = convection coefficient, W/m^2 K
H = h/k
k = thermal conductivity of the cylinder, W/m K
K_n = nth kernel
L = length of cylinder, m
λ_n = nth eigenvalue
r = radial direction of the cylinder
t = time, seconds
$T(z,t)$ = Wall temperature at location z and at time t
T_∞ = ambient temperature
θ = difference between the cylinder wall temperature and the ambient temperature, °C
$\bar{\theta}$ = transformed θ
w = wall thickness of the cylinder, m
z = axial direction of the cylinder
z_0 = initial position of the tool, m

References

[1] Subramani, G., Kapoor, S. G., and DeVor, R. E., 1993, ''A Model for the Prediction of Bore Cylindricity During Machining,'' ASME J. Eng. Ind., **115**, pp. 15–22.
[2] Zhang, G. M., and Kapoor, S. G., 1985, ''Dynamic Modeling and Analysis of the Boring Machine System,'' *Proc. of the ASME Symposium on Sensors and Controls for Manufacturing*, PED-**18**, pp. 11–20.
[3] Subramani, G., Suvada, R., Kapoor, S. G., DeVor, R. E., and Meingast, W., 1987, ''A Model for the Prediction of Force System for Cylinder Boring Process,'' *Proc. of the 15th North Amer. Manf. Res. Conf.*, pp. 439–446.
[4] Sutherland, J. W., Subramani, G., Kuhl, M. J., DeVor, R. E., and Kapoor, S. G., 1988, ''An Investigation into the Effect of Tool and Cut Geometry on Cutting Force System Prediction Models,'' *Proc. of the 16th North Amer. Manf. Res. Conf.*, pp. 264–272.
[5] Childs, T. H. C., Maekawa, K., and Maulik, P., 1998, ''Effects of Coolant on Temperature Distribution in Metal Cutting,'' Mater. Sci. Technol., **4**, pp. 1006–1019.
[6] Incropera, F. P., and DeWitt, D. P., 1990, *Introduction to Heat Transfer*, 2nd ed., Wiley, New York.
[7] Rapier, A. C., 1954, ''A Theoretical Investigation of the Temperature Distribution in the Metal Cutting Process,'' Br. J. Appl. Phys., **5**, November, pp. 400–405.
[8] Weiner, J. H., 1955, ''Shear Plane Temperature Distribution in Orthogonal Cutting,'' Trans. ASME, **77**, No. 8, pp. 1331–41.
[9] Subramani, G., Whitmore, M. C., Kapoor, S. G., and DeVor, R. E., 1991, ''Temperature Distribution in a Hollow Cylindrical Workpiece During Machining: Theoretical Model and Experimental Results,'' ASME J. Eng. Ind., **113**, No. 4, pp. 373–380.
[10] Yen, D. W., and Wright, P. K., 1986, ''Remote Temperature Sensing Technique for Estimating the Cutting Interface Temperature Distribution,'' ASME J. Eng. Ind., **108**, pp. 252–263.
[11] Chow, J. G., and Wright, P. K., 1988, ''On-line Estimation of Tool/Chip Interface Temperature for a Turning Operation,'' ASME J. Eng. Ind., **110**, pp. 56–64.
[12] Watts, R. G., and McClure, E. R., 1968, ''Thermal Expansion of Workpiece During Turning,'' *ASME Paper*, No. 68-WA/Prod-24.
[13] Watts, R. G., 1969, ''Temperature Distributions in Solid and Hollow Cylinders Due to a Moving Circumferential Ring Heat Source,'' J. Heat Transfer, **91**, pp. 465–470.
[14] Ichimiya, R., and Kawahara, H., 1971, ''Investigation of Thermal Expansion in Machining Operations,'' Bull. JSME, **14**, No. 78, pp. 1363–1371.
[15] Stephenson, D., 1991, ''An Inverse Method for Investigating Deformation Zone Temperatures in Metal Cutting,'' ASME J. Eng. Ind., **113**, pp. 129–136.
[16] Stephenson, D., Barone, M., and Dargush, G., 1995, ''Thermal Expansion of the Workpiece in Turning,'' ASME J. Eng. Ind., **117**, pp. 542–550.
[17] Kakade, N. N. and Chow, J. G., 1989, ''Computer Simulation of Bore Distortions for Engine Boring Operation,'' *Proc. of the Symp. on Collected Papers in Heat Transfer*, Winter Annual Meeting, San Francisco, CA, Vol. 123, pp. 259–265.
[18] Ozisik, M. N., 1968, *Boundary Value Problems of Heat Conduction*, International Textbook Company.
[19] Cozzens, D. A., 1995, *A Study of Cutting Fluids and Workpiece Surface Error in the Boring of Cast Aluminum Alloys*, M. S. Thesis, Michigan Technological University.
[20] Jacobus, K. J., DeVor, R. E., and Kapoor, S. G., 1999, ''Part Warpage Model Based on Machining-Induced Residual Stress,'' Trans. NAMRI/SME, **27**, pp. 75–80.
[21] Fuh, K. H., Ching-Fu, Wu, 1995, ''A Residual-Stress Model for the Milling of Aluminum Alloy (2014-T6),'' J. Mater. Process. Technol., **51**, pp. 87–105.
[22] Ozisik, M. N., 1980, *Heat Conduction*, Wiley, New York.